Synthesis, structures, and spectroscopic properties of Hg(II) complexes of bidentate NN and tridentate NNO Schiff-base ligands

Basu Baul, Tushar S ; Kundu, Sajal ; Höpfl, Herbert ; Tiekink, Edward R T ; Linden, Anthony

Abstract: Reactions of HgX2 (X = Cl, N3, NO3) with (E)-2-methoxy-N-(pyridin-2-ylmethylene)aniline (L1) and (E)-4-methoxy-N-(pyridin-2-ylmethylene)aniline (L2) in ethanol gave two monomers, [HgL1(Cl)2] (1) and [HgL2(NO3)2(DMSO)] (5), and three coordination polymers, [HgL1(N3)2]2 · Hg(N3)2n (2), [HgL2(Cl)2]n (3), and [HgL2(NO3)2]n · nCH3CN (4). Compounds 1–5 were characterized by elemental analysis, IR, NMR spectroscopy, and single-crystal X-ray diffraction. The common feature of monomeric 1 and 5 is the presence of intra- and intermolecular Hg–O bonds. In the absence of these, polymeric structures arise as a result of azide, chloride, and nitrate bridging in 2, 3, and 4, respectively. Fluorescent properties of 1–5 were also investigated.

DOI: https://doi.org/10.1080/00958972.2014.901508

Synthesis, structures and spectroscopic properties of Hg(II) complexes of bidentate NN and tridentate NNO donor Schiff-base ligands

TUSHAR S. BASU BAUL[a, *], SAJAL KUNDU[a], HERBERT HÖPFL[b], EDWARD R. T. TIEKINK[c, *], ANTHONY LINDEN[d]

[a]Centre for Advanced Studies in Chemistry, North-Eastern Hill University, NEHU Permanent Campus, Umshing, Shillong 793 022, India

[b]Centro de Investigaciones Químicas, Universidad Autónoma del Estado de Morelos, Av. Universidad 1001, 62209 Cuernavaca, Mexico

[c]Department of Chemistry, University of Malaya, 50603 Kuala Lumpur, Malaysia

[d]Department of Chemistry, University of Zurich, Winterthurerstrasse 190, CH-8057 Zurich, Switzerland

ABSTRACT

Reactions of HgX_2 (X = Cl, N_3, NO_3) with (*E*)-2-methoxy-N-(pyridin-2-ylmethylene)aniline (L^1) and (*E*)-4-methoxy-N-(pyridin-2-ylmethylene)aniline (L^2) in ethanol gave rise to two monomers $[HgL^1(Cl)_2]$ (**1**) and $[HgL^2(NO_3)_2(DMSO)]$ (**5**), and three coordination polymers $\{[HgL^1(N_3)_2]_2{\cdot}Hg(N_3)_2\}_n$ (**2**), $[HgL^2(Cl)_2]_n$ (**3**) and $[HgL^2(NO_3)_2]_n{\cdot}nCH_3CN$ (**4**). Compounds **1**-**5** were characterized by elemental analysis, IR, NMR and single-crystal X-ray diffraction. The common feature of monomeric structures in compounds **1** and **5** is the presence of intra- and inter-molecular Hg-O bonds. In the absence of these, polymeric structures arise as a result of

azide, chloride and nitrate bridging in compounds **2**, **3** and **4**, respectively. In addition, the fluorescent properties of **1**-**5** were also investigated.

Keywords: Synthesis / Mercury(II) compounds / *N*,*N*-donor ligands / Photophysical properties / Crystal structures

---

* Corresponding authors. *E-mail addresses*: basubaul@nehu.ac.in, basubaulchem@gmail.com (T. S. Basu Baul), Edward.Tiekink@gmail.com (Edward R. T. Tiekink)

1. Introduction

Schiff-base ligands and their metal complexes have received attention owing to their distinctive coordination and structural properties [1-5]. In addition, Schiff-base compounds of transition metals have become important components for the generation of supramolecular aggregates through the formation of coordination bonds, hydrogen bonding and other intermolecular interactions, thereby creating a large variety of supramolecular architectures including high-dimensional frameworks [6-9]. Recent X-ray crystallographic studies performed on a variety of mercury(II) compounds derived from Schiff-base ligands, *viz.* $HgLX_2$, $[HgLX_2]_2$, $[HgLX_2]_n$ and $\{[HgLX_2]_2\}_n$ with L = variously substituted (*E*)-*N*-(pyridin-2-ylmethylene)arylamine and X = halides or pseudohalides or nitrates, revealed that mercury(II) compounds are promising candidates for the generation of interesting and diverse supramolecular assemblies [10,11]. Although the global topology (monomer, dimer, polymer, etc.) of the resulting compound is determined by the interplay between Hg^{2+}, X^-, and L, in the solid-state, the crystal structure is frequently controlled by weaker intermolecular interactions such as π–π and CH–π contacts.

Herein, we report on the synthesis and solid-state structures of five new mercury(II) compounds derived from (*E*)-2-methoxy-N-(pyridin-2-ylmethylene)aniline (L^1) and (*E*)-4-methoxy-N-(pyridin-2-ylmethylene)aniline (L^2), which have been prepared from HgX_2 (X = Cl, N_3 and NO_3) (Scheme 1) and then characterized by using spectroscopic methods and single-crystal X-ray diffraction analysis. The structural characterization evidenced the formation of either mononuclear or polymeric compounds. The coordination numbers range from 4 to 8 which are not systematically correlated to L^1/L^2 or X or solvent.

2. Experimental

2.1. Materials, Methods and Instruments

Caution! *Mercury compounds are highly toxic* [12]. *Care must be taken when handling samples, and appropriate disposal procedures are necessary.* All chemicals were used as purchased without purification: $HgCl_2$, NaN_3, pyridine-2-carboxaldehyde (Merck), $Hg(NO_3)_2$ (Sarabhai Chemicals), $Hg(OAc)_2$, *o*-anisidine, *p*-anisidine (Sd fine). (*E*)-2-methoxy-N-(pyridin-2-ylmethylene)aniline (L^1) and (*E*)-4-methoxy-N-(pyridin-2-ylmethylene)aniline (L^2) were generated *in situ* from pyridine-2-carboxaldehyde and the corresponding anisidine. Solvents were purified by standard procedures and were freshly distilled prior to use. Melting points were recorded in capillary tubes on a Scanca apparatus and are uncorrected. Elemental analyses were performed using a Perkin Elmer 2400 series II instrument. IR spectra in the range 4000-400 cm^{-1} were obtained on a Perkin Elmer Spectrum BX series FT-IR spectrophotometer with samples investigated as KBr discs. ^1H NMR spectra were recorded on a Bruker Avance II spectrometer and measured at 400.13 MHz, and the chemical shifts were referenced to Me_4Si set at δ 0.00 ppm; the numbering scheme is as shown in Scheme 1. Steady-state absorption spectra were recorded at ambient temperature in acetonitrile (spectroscopy grade, Merck) solution on a Perkin-Elmer model Lambda25 absorption spectrophotometer. Fluorescence spectra were obtained on a Hitachi model FL4500 spectrofluorimeter (with the excitation and emission slits fixed at 10 and 20 nm, respectively). All spectra were corrected for the instrument response function. Quartz cuvettes of 10 mm optical path length received from Perkin Elmer, USA (part no. B0831009), and Hellma, Germany (type 111-QS), were used for measuring absorption and fluorescence spectra, respectively. Fluorescence quantum yields (ϕ_f) were calculated by comparing the total fluorescence intensity over the whole fluorescence spectroscopic range with that of a standard using the method described elsewhere [10]. The relative experimental error of

the measured quantum yield was estimated within ±10%. Solution electrical conductivity measurements were made in acetonitrile with a Wayne Kerr automatic precision bridge 6440B.

2.2. Synthesis of mercury compounds

2.2.1. Synthesis of $[HgL^1(Cl)_2]$ (1). To a solution of pyridine-2-carboxaldehyde (0.13 g, 1.21 mmol) in ethanol (5 mL) was added a solution of *o*-anisidine(0.15 g, 1.21 mmol) in ethanol (5 mL). After stirring the reaction mixture at ambient temperature for 30 min., a solution of $HgCl_2$ (0.33 g, 1.21 mmol) in methanol (20 mL) was added drop-wise, which resulted in the formation of a yellow precipitate. Stirring was continued for 3 h and then the mixture was filtered. The solid residue was washed with methanol (3 x 5 mL), dried *in vacuo* and then dissolved in 40 mL of hot acetonitrile. The solution was filtered while hot and upon cooling to room temperature, a yellow crystalline material was obtained. Yield 0.35 g (40%). M.p. 172-173 °C. Anal.Calc. for $C_{13}H_{12}Cl_2HgN_2O$ (MW 483.74): C, 32.28; H, 2.50; N, 5.79. Found: C, 32.60; H, 2.62; N, 5.80%. Λ_m (CH_3CN): 6 $\Omega^{-1}cm^2mol^{-1}$. IR (cm^{-1}): 1623 w, 1588 s: ν(C=N_{imine}+ C=N_{py}), 1563 w, 1492 s, 1475 w, 1462 m, 1438 w: ν(C=N_{py}), 1368 m, 1286 w, 1269 m, 1250 vs, 1178 w, 1156 w, 1156 m, 1117 vs, 1047 w, 1021 m, 1011 w, 972 w, 958 w, 942 w, 903 w, 774 vs, 759 w, 744 w, 638 w, 617 w, 537 w, 508 w. ^{1}H-NMR (DMSO-d_6): 9.23 [s, 1H, H-7], 8.79 [d, 1H, H-3′], 8.19 [m, 2H, H-5′,6′], 7.84 [t, 1H, 4′], 7.60 [d, 1H, H-4], 7.43 [t, 1H, H-6], 7.10 [m, 2H, H-3,5], 4.0 [s, 3H, OCH_3] ppm.

2.2.2. Synthesis of $\{[HgL^1(N_3)_2]_2{\cdot}Hg(N_3)_2\}_n$ (2). *Note: While no incident occurred while using azide during preparation and isolation, care in handling azides must be exercised owing to their potentially explosive nature.* To a solution of pyridine-2-carboxaldehyde (0.25 g, 2.33 mmol) in ethanol (5 ml) was added a solution of *o*-anisidine (0.28 g, 2.32 mmol) in ethanol (5 mL). The mixture was stirred at ambient temperature for 30 min and then added drop-wise to a methanolic solution containing HgN_3, which was prepared *in situ* from $Hg(OAc)_2$ (1.11 g, 3.48 mmol) in methanol (50 mL) and NaN_3 (0.68 g, 10.46 mmol) in 40 mL of the same solvent. Immediate

formation of a yellow precipitate occurred. Stirring was continued for 4 h and then the mixture was filtered. The residue was washed thoroughly with water, then with methanol (3 x 5 mL) and dried *in vacuo*. The dried solid was dissolved in 60 mL of hot acetonitrile and filtered while hot. Upon cooling to room temperature, a yellow crystalline material was obtained. Yield 0.39 g (56%). M.p. 145-146 °C. Anal. Calc. for $C_{26}H_{24}Hg_3N_{22}O_2$ (MW 1278.39): C, 24.43; H, 1.89; N, 24.10. Found: C, 24.66; H, 1.80; N, 23.92%. Λ_m (CH_3CN): 5 $\Omega^{-1}cm^2mol^{-1}$. IR (cm^{-1}): 2037 vs: $\nu_{as}(N_3)$, 1623 s: $\nu(C{=}N_{imine})$, 1589 m, 1496 m, 1471 w, 1458 w: $\nu(C{=}N_{py})$, 1434 w, 1371 m, 1287 w, 1272 w, 1253 s, 1193 w, 1149 w, 1119 vs, 1053 w, 1021 m, 1011 w, 972 w, 952 w, 932 w, 901 w, 773 m, 754 w, 637 w, 535 w, 505 w. ^{1}H-NMR (DMSO-d_6): 8.94 [s, 1H, H-7], 8.73 [d, 1H, H-3´], 7.98 [m, 2H, H-5´,6´], 7.59 [t, 1H, 4´], 7.33 [d, 1H, H-4], 7.28 [t, 1H, H-6], 6.98 [m, 2H, H-3,5], 3.92 [s, 3H, OCH_3] ppm.

2.2.3. Synthesis of $[HgL^2(Cl)_2]_n$ (3). A similar synthetic procedure as for **1** was used except that *o*-anisidine was replaced by *p*-anisidine, giving yellow crystals after recrystallization from acetonitrile. Yield 0.30g (49%). M.p. 192-193 °C. Anal. Calc. for $C_{13}H_{12}Cl_2HgN_2O$ (MW 483.74): C, 32.28; H, 2.50; N, 5.79. Found: C, 32.35; H, 2.42; N, 6.07%. Λ_m (CH_3CN): 7 $\Omega^{-1}cm^2mol^{-1}$. IR (cm^{-1}): 1621 w: $\nu(C{=}N_{imine})$, 1596 s, 1505 vs, 1473 w, 1434 w: $\nu(C{=}N_{py})$, 1307 m, 1251 vs, 1171 m, 1029 vs, 835 s, 776 s, 537 m. ^{1}H-NMR (DMSO-d_6): 9.05 [s, 1H, H-7], 8.93 [d, 1H, H-3´], 8.13 [d, 2H, H-5´,6´], 7.75 [t, 1H, 4´], 7.65 [d, 2H, H-2,6], 7.00 [d, 2H, H-3,5], 3.85 [s, 3H, OCH_3] ppm.

2.2.4. Synthesis of $[HgL^2(NO_3)_2]_n{\cdot}nCH_3CN$ (4). $Hg(NO_3)_2$ (0.60 g, 1.46 mmol) was dissolved under heating in five drops of concentrated nitric acid and the resulting solution was diluted with

water (10 mL). This mixture was added drop-wise to a solution containing pyridine-2-carboxaldehyde (0.155 g, 1.45 mmol) and *p*-anisidine (0.179 g, 1.45 mmol) in ethanol (10 mL), which resulted in the immediate formation of a yellow precipitate. Stirring was continued for 3 h and then the mixture was filtered. The residue was washed thoroughly with water until the filtrate was pH neutral, then with methanol (3 x 5 mL) and dried *in vacuo*. The dried solid was dissolved in 60 mL of hot acetonitrile and filtered while hot. The filtrate upon cooling to room temperature afforded compound **4** in the form of a pale yellow crystalline material. Yield 0.50 g (56%). M.p. 150-151°C. Anal. Calc. for $C_{15}H_{15}HgN_5O_7$ (MW 577.90): C, 31.18; H, 2.62; N, 12.12. Found: C, 31.20; H, 2.42; N, 11.90%. Λ_m (CH_3CN): 9 $\Omega^{-1}cm^2mol^{-1}$. IR (cm^{-1}) KBr: 1623 w: ν(C=N_{imine}), 1594 s, 1559 m, 1507 s, 1496 m, 1447 w: ν(C=N_{py}), 1384 vs, 1306 w: $\nu(NO_3)$, 1257 vs, 1172 m, 1117 w, 1018 m, 984 m, 831 s, 776 m, 743 w, 612 w, 539 w, 518 w; Nujol: 1593 ν(C=N_{imine} + C=N_{py}), 1527 $\nu_1(NO_3)$, 1314 $\nu_5(NO_3)$. ^{1}H-NMR (DMSO-d_6): 9.35 [d, 1H, H-3´], 8.93 [s, 1H, H-7], 8.40 [t, 1H, H-5´], 8.23 [d, 1H, 6´], 8.03 [t, 1H, H-4´], 7.52 [d, 1H, H-2,6], 6.97 [d, 2H, H-3,5], 3.84 [s, 3H, OCH_3] ppm.

2.2.5. Synthesis of [$HgL^2(NO_3)_2$(DMSO)] (5). Crystallization of **4** in a solvent mixture of DMSO and chloroform (1:4, *v*/*v*) afforded pale-yellow crystals of compound **5** in 56% yield. M.p. 165-166 °C. Anal. Calc. for $C_{15}H_{18}HgN_4O_8S$: C, 29.28; H, 2.95; N, 9.11. Found: C, 29.50; H, 3.08; N, 9.10%. Λ_m (CH_3CN): 9 $\Omega^{-1}cm^2mol^{-1}$. IR (cm^{-1}) KBr: 1621 w: ν(C=N_{imine}), 1595 m: ν(C=N_{py}), 1579 w, 1559 w, 1507 m, 1384 vs: $\nu(NO_3)$, 1320 w, 1308 w, 1254 vs, 1170 m, 1158 w, 1103 w, 1021 s: ν(S=O), 948 m, 831 s, 781 m, 639 w, 537 w. ^{1}H-NMR (DMSO-d_6): 9.34 [d, 1H, H-3´], 8.95 [s, 1H, H-7], 8.39 [t, 1H, H-5´], 8.29 [d, 1H, 6´], 8.00 [t, 1H, H-4´], 7.55 [d, 1H, H-2,6], 7.02 [d, 2H, H-3,5], 3.84 [s, 3H, OCH_3], 3.46 [s, 6H, $(CH_3)_2SO$)] ppm.

2.3. X-ray data collection and structure determination

Crystals suitable for single-crystal X-ray diffraction analysis were obtained from acetone/acetonitrile (**1**), acetonitrile (**2-4**) and a solvent mixture of dimethylsulfoxide and chloroform (**5**), by slow evaporation of the solvent at room temperature. The crystal for **1** was investigated at room temperature on a Bruker APEX diffractometer equipped with a CCD area detector (Mo Kα radiation with λ = 0.71073 Å, graphite monochromator). Data for **2** and **3** were recorded at low temperature on an Agilent Technologies Super Nova area-detector diffractometer [13] using Mo Kα radiation (λ = 0.71073 Å) from a micro-focus X-ray source and an Oxford Instruments Cryojet XL cooler. The measurements for **4** and **5** were made at low temperature on a Nonius KappaCCD diffractometer [14] with graphite-monochromated Mo Kα radiation (λ = 0.71073 Å) and an Oxford Cryosystems Cryostream 700 cooler. Data reduction was performed with SAINT [15] for **1**, with CrysAlisPro [13] for **2** and **3**, and HKL Denzo and Scalepack [16] for **4** and **5**. Intensities were corrected for Lorentz and polarization effects. An empirical absorption correction based on the multi-scan method [17] was applied for **1**, **4** and **5**, the data for **3** were treated with an empirical absorption correction using spherical harmonics [13], and for **2** an analytical absorption correction [18] was employed. Relevant data collection and refinement parameters are given in Table 1, and perspective views of the structures are shown in Figs. 2a, 3a-7a. The structures of compounds **1**, **4** and **5** were solved by heavy-atom Patterson methods [19] which revealed the position of the mercury atom in their respective compounds. The structures of **2** and **3** were solved by direct methods using SHELXS97 [20], giving the positions of all non-hydrogen atoms. In **1**, the asymmetric unit consists of two independent mononuclear complex molecules. The asymmetric unit in **4** contains one chemical

repeat unit of the Hg-complex polymer plus one molecule of MeCN. The refinement of the structures was carried out on F^2 by using full-matrix least-squares procedures, which minimized the function $\Sigma w(F_o^2 - F_c^2)^2$. The non-hydrogen atoms in each structure were refined anisotropically. All of the H-atoms were placed in geometrically calculated positions and refined by using a riding model where each H-atom was assigned a fixed isotropic displacement parameter with a value equal to $1.2U_{eq}$ of its parent atom ($1.5U_{eq}$ for any methyl group). A correction for secondary extinction was applied for **4** and **5**. For **1** (three reflections) and for **4** and **5** (one reflection each) were omitted from the final refinement as the intensities were considered to be extreme outliers. The structure of **5** was refined as an inversion twin in which the major twin fraction was 0.859(1). With the exception of the positive residual electron density peaks, Table 1, in **3** (1.18 Å from Cl2) and **4** (1.24 Å from C2), the maximum and minimum residual electron density peaks in the final difference maps were located in the vicinity of a mercury(II) atom. Refinement and data output of **1** was carried out with the SHELXTL-NT program package [20] while the SHELXL97 program [21] was used for the calculations of **2-5**. All crystallographic figures were drawn using SHELXTL-NT [20] or DIAMOND [22].

3. Results and discussion

3.1. Syntheses

The reactions for the formation of the mercury Schiff base compounds **1**, **3** and **4** were carried out in methanol or ethanol using 1:1 stoichiometric ratios. In either solvent, one equivalent of HgX_2 (X = Cl, NO_3) reacts rapidly with one equivalent of L (generated *in situ* from pyridine-2-carboxaldehyde and *o/p*-anisidine) to give a yellow precipitate, from which mercury(II)

compounds of the formulae $[HgL^1(Cl)_2]$ (**1**), $[HgL^2(Cl)_2]_n$ (**3**) and $[HgL^2(NO_3)_2]_n{\cdot}nCH_3CN$ (**4**) were isolated. The combination of compound **4** with DMSO as a donor ligand resulted in the formation of $[HgL^2(NO_3)_2(DMSO)]$ (**5**). Earlier, it was demonstrated that the reaction of one equivalent of $Hg(N_3)_2$ with one equivalent of L, where L = (*E*)-4-methyl-N-(pyridin-2-ylmethylene)aniline, gives a yellow product of the composition $\{[HgL(N_3)_2]_2\}_n$ [10]. Now, a compound of the composition $\{[HgL^1(N_3)_2]_2{\cdot}Hg(N_3)_2\}_n$ (**2**) was isolated from a reaction of L^1 with an excess of $Hg(N_3)_2$. Compound **2** is trinuclear and can be considered as an adduct formed between a dimeric $[HgL^1(N_3)_2]_2$ complex and $Hg(N_3)_2$. Compounds **1**-**5** are air-stable and behave as non-electrolytes in acetonitrile solution (see *section 2.2*). The structures and geometries of compounds **1**-**5** are detailed in Scheme 1. The results of the crystal structure determinations of **1**-**5** (see *section 3.3*) are consistent with the chemical and spectroscopic analyses.

3.2. IR, NMR, UV-Vis and fluorescence spectroscopy

The infrared spectroscopic assignments of selected diagnostic bands for compounds **1**-**5** are given in *section 2.2*. All compounds display a moderately intense band in the region of 1590-1620 cm^{-1}, which is characteristic for the $\nu(C{=}N_{imine})$ stretch of the metal-coordinated Schiff base ligands [10,11,23]. In addition, well-resolved sharp bands of variable intensity observed in the regions 1600-1580, 1490-1475 and 1450-1435 cm^{-1} were assigned to metal-coordinated pyridine rings [10,11,23-25]. The azide and nitrate compounds **2**, **4** and **5** deserve further specific mention. A noteworthy observation for **2** is the appearance of a very strong band at 2037 cm^{-1} corresponding to $\nu_{as}(N_3)$ [26,27]. A similar observation was recently noted for the cognate compound $\{[HgL(N_3)_2]_2\}_n$, where L = (*E*)-4-methyl-*N*-(pyridin-2-ylmethylene)aniline [10]. On the other hand, complex **4** displays a strong band at approximately 1384 cm^{-1}, which is indicative

of the simultaneous presence of non-coordinated and coordinated nitrate anions [24,28]. The KBr spectrum of **4** also displayed bands at 1507 and 1306 cm^{-1}, which are indicative of bidentate chelating nitrate groups. The assumption of bidentate chelating nitrate groups [24] was further confirmed from the spectrum of **4** run in Nujol mull, giving bands at 1527 cm^{-1} for $\nu_1(NO_3)$ and at 1314 cm^{-1} for $\nu_5(NO_3)$, corresponding to a difference of $\Delta(NO_3)$ = 213 cm^{-1} [29]. A similar observation was made recently for an analogous mercury compound, $[HgL(NO_3)_2]_n$, which has also been characterized crystallographically [10]. In addition to bands for the vibration of nitrate groups, compound **5** displayed a strong band at 1021 cm^{-1}, which can be attributed to ν(S=O) of DMSO coordinated to a mercury(II) atom. This value is 35 cm^{-1} lower than that reported for free DMSO (1055 cm^{-1}) and is thus indicative of a terminal (end-on) O-monocoordination. It should be noted that for S-bonded DMSO, an increase of the frequency would be expected [30,31]. Thus, the IR spectroscopic data provided substantial evidence in support of the structures and the postulations were subsequently confirmed by single crystal X-ray crystallography (see *section 3.3*).

The ^{1}H NMR spectra in DMSO-d_6 solution displayed the expected signals, which correlate well with the hydrogen atoms present in the molecules. Coupling constants could not be established with certainty owing to the broad unresolved nature of the signals. The NMR assignments for the compounds presented in the *Experimental section* are based on the splitting patterns of the signals and by comparing the data with those in previous reports [32,33].

Table 2 summarizes the UV-vis and fluorescent properties of compounds **1**-**5**. The electronic spectra exhibited a strong absorption in the range of 350-380 nm (Figure 1a) which is possibly a result of overlap of intramolecular charge transfer transitions ($\varepsilon \sim 10^4$) with a weak MLCT transition from Hg(II) $\rightarrow \pi^*$ (ligand) [10,11]. In acetonitrile solution, compounds display broad

emission bands at approximately λ_{max} = 410 nm along with a shoulder at ~ 430 nm, except for an additional band at 502 nm for **1**, when they are excited at their respective absorption maxima (Figure 1b), indicating the charge transfer nature of the transitions [10,11]. Compounds **1-5** show very low fluorescent quantum yields (ϕ_F), which can be attributed to the heavy atom effect [34,35] and the ϕ_F values were of the same order of magnitude as observed recently for related systems [10,11]. No appreciable change in ϕ_F was noticed according to the variation of the substituents in the ligands from 2-OCH_3 (**1** and **2**) to 4-OCH_3 (**3-5**) or according to the variation of the anion (chloride, azide and nitrate).

3.3. Single-crystal X-ray diffraction studies

The crystal structures of **1-5** were established by X-ray crystallography which revealed the presence of monomeric (**1**, **3** and **5**) and polymeric (**2** and **4**) species in the solid-state. Two independent monomers comprise the asymmetric unit of **1** which, to a first approximation are similar (Figs 2a and 2b); geometric parameters for the first independent molecule of **1** are collated in Table 3. The mercury(II) atom is five-coordinate being bound by a tridentate L^1 ligand which chelates the metal atom via the nitrogen atoms while simultaneously forming a Hg□O bond; the coordination environment is completed by two chloride ligands. As observed in related structures [10,11], the Hg-N(pyridyl) bond length is shorter than the Hg-N(imine) bond. The chelate ring is planar in both molecules, exhibiting a r.m.s. deviation of 0.016 and 0.029 Å, respectively. However, this planarity does not extend over the entire L^1 ligand as seen in the dihedral angles formed between the outer six-membered rings of 32.2(5) and 29.5(4)º, respectively, there being a twist about the imine-N□C(methoxyphenyl) bond; the C6-N2-C7-C8 and C26-N22-C27-C28 torsion angles are 29.3(12) and 23.0(11)º, respectively. This difference

between the independent molecules is highlighted in the overlay diagram [36] (Figure 3a). Similar ligand conformations are found in **2**-**5**. Based on the value of $\tau = 0.23$, the trigonality index [37], compared with 0.0 and 1.0 for ideal square pyramidal and trigonal bipyramidal geometries, respectively, the coordination geometry about the Hg1 atom is based on a square pyramid. The comparable value for the second molecule is 0.02, suggesting a more regular coordination geometry. The greater distortion for the Hg1 atom is traced to a secondary Hg1...Cl21^{i} interaction of 3.309(2) Å (symmetry operation i: -1+*x*, -1+*y*, *z*) between the independent molecules as shown in (Figure 3b). Often molecules related to **1** dimerise about a centre of inversion via Hg...Cl bridges to form binuclear arrangements [10,11]. In the case of **1**, the presence of Hg-O bonds reduced the Lewis acidity of the mercury(II) atom and only a single and weak Hg...Cl contact between the molecules is formed instead. Also highlighted in Figure 3b, is the presence of a pyridyl-C-H...Cl hydrogen bond [H...Cl = 2.79 Å]. In the crystal structure of **1**, there are two such pyridyl-C-H...Cl interactions and these, coupled with the Hg...Cl interaction, serve to link the molecules into an array in the bc-plane. A three-dimensional architecture arises from π-π interactions along the a-direction between centrosymmetrically related N21-pyridyl rings, and between N21-pyridyl and $Hg1N_2C_2$ chelate rings (Figure 3c). The latter π-π interactions where a chelate ring defines a π-system are known in the literature [38-40] and indeed, have been seen in related structures [10,11].

The structure of $\{[HgL^1(N_3)_2]_2 \cdot Hg(N_3)_2\}_n$ (**2**) is best described a comprising a $Hg(N_3)_2$unit and a centrosymmetric dimer of $[HgL^1(N_3)_2]_2$ with links between them provided by azido-N atoms, Figure 4. The Hg2 atom in $Hg(N_3)_2$ is located on a centre of inversion and is bound by two terminally-bound azido-N9 atoms, two μ_2-azido-N atoms, where the atom N6 bridges across to Hg1, and two azido-N5 atoms, where the azido-N3 atom at the other end provides the bridge

between the Hg1 atoms of the centrosymmetric dimer, hence this ligand is a μ_3-bridging. In the dimer, atoms Hg1 and Hg1' are connected by a pair of end-on bridging azide molecules, via N3 and N3' (the N5 atoms of these azides form bridges to the Hg2 atoms in the $Hg(N_3)_2$units), the second azido-N6 is bound end-on and bridges to an adjacent Hg2, and tridentate L^1coordinates as found in **1**. The Hg1 and Hg2 atoms exist in octahedral coordination geometries, at least to a first approximation. For Hg1, two of the bond lengths are considerably longer than the others, e.g. the central core is trapezoidal as the Hg1-N3,N3' bond lengths differ by about 0.6 Å, and the Hg-O1 distance is also long, Table 4. Further distortions arise as a result of the acute chelate angles. While the angles around Hg2 are close to 90º, Table 4, two of the Hg-N9 bond lengths are considerably shorter, by over 0.7 Å, than the remaining four bonds. The result of the azide-mediated bridging is the formation of a coordination polymer aligned along the a-axis. Chains stack with no specific intermolecular interactions between them.

The next structure to be described is that of $[HgL^2(Cl)_2]_n$ (**3**) where the methoxy substituent is no longer proximate to the mercury(II) atom so that a Hg-O1 bond is not formed. Instead, the mercury(II)atom increases its coordination number leading to a square pyramidal coordination geometry (τ = 0.02, Cl2 in the axial position) by forming a significant intermolecular Hg1...Cl2 interaction (2.7874(11) Å for symmetry operation 1-*x*, ½+*y*, 1½-*z*) resulting in a helical supramolecular chain along the b-axis, Figure 5a. The chains are connected by C8-H...Cl2 hydrogen bonds as well as π-π interactions between pyridyl and phenyl rings to form a supramolecular array in the ab-plane, Figure 5b. Layers stack with no specific intermolecular interactions between them.

The mercury(II) atom in polymeric $[HgL^2(NO_3)_2]_n{\cdot}nCH_3CN$ (**4**), Figure 6a, is eight-coordinate being chelated by L^2, and coordinated by six nitrate-O atoms. The N3-nitrate chelates

in an asymmetric mode with the Hg-O3 bond length being 0.6 Å shorter than Hg-O2, Table 5. The N4-nitrate bridges two mercury(II) atoms, simultaneously chelating both with the O5 atom forming two Hg-O bonds. Reflecting the higher denticity of the N4-nitrate anion, the Hg-O bond lengths are long and span a range 2.587(4) to 2.924(4) Å. The disparity in the bond lengths about the mercury(II) atom along with the acute chelate angles leads to a highly distorted coordination geometry. One description is based on a square anti-prism with one face (distinctly rectangular, defined by the O2, O3, O5' and O6 atoms) being twisted about 7º by with respect to the other (distinctly trapezoidal, defined by O5, O7, N1 and N2). The result of the tetradentate and bridging N4-nitrate ligand is the formation of a helical coordination polymer along the b-axis as illustrated in Figure 6b. When viewed down the direction of the polymer, the global crystal packing can be described in terms of undulating layers of polymers stacked along the c-axis, Figure 6c, and the solvent acetonitrile molecules lie in the inter-layer region. Connections within layers are of the type methyl-C-H...O(nitrate), as are those between the solvent and layer.

The recrystallisation of **4** from DMSO yielded **5**, formulated as $[HgL^2(NO_3)_2(DMSO)]$, which is monomeric and features O-bound DMSO, Figure 7a. Both nitrate anions are chelating with the Hg-O bond lengths spanning a range 2.393(3) to 2.712(3) Å, i.e. within the range of comparable bonds in **4**, Table 5. The L^2 ligand is also chelating and the Hg-N1, N2 bond lengths are longer than those in **4**, reflecting the more tightly bound nitrates but also the strong Hg-O8 bond of 2.229(3) Å involving the DMSO-O atom. With three acute angles provided by the chelating ligands, not surprisingly the coordination is highly distorted. One description is based on a capped octahedron. The axial angle of 160.11(11) is subtended by the O5 and N2 atoms, the approximate basal plane is defined by the O2, O3, O8 and N1 atoms leaving the O7 atom to occupy the triangular face defined by the O5, O8 and N1 atoms. In the crystal packing, a pair of

π-π interactions occurring between the pyridyl and phenyl rings of centrosymmetrically related molecules leads to the formation of loosely associated dimeric units. The dimeric aggregates stack in columns along the a-axis and are connected into a three-dimensional architecture by C-H...O interactions, Figure 7b, involving nitrate-O as acceptors, as for **4**, the methoxy-O as an acceptor, and L^2- and DMSO-methyl-H as donors.

4. Conclusions

Five neutral $[HgL^1(Cl)_2]$ (**1**), $\{[HgL^1(N_3)_2]_2{\cdot}Hg(N_3)_2\}_n$ (**2**), $[HgL^2(Cl)_2]_n$ (**3**), $[HgL^2(NO_3)_2]_n{\cdot}nCH_3CN$ (**4**), and $[HgL^2(NO_3)_2(DMSO)]$ (**5**) compounds of bidentate NN and tridentate NNO donor Schiff-base ligands have been synthesised. The compounds were characterised by spectroscopic and single crystal X-ray crystallographic techniques. The crystal structures revealed the presence of monomeric (**1**, **3** and **5**) and polymeric (**2** and **4**) species in the solid-state. The appearance of monomeric **1** and **5** is correlated with the additional coordination, intra- and intermolecularly, by oxygen which reduces the Lewis acidity of the mercury(II) centre. In the absence of additional Hg–O bonds, polymeric structures arise, via bridging azide, chloride and nitrate in the structures of **2**, **3** and **4**, respectively.

Supplementary material

CCDC 970664-970668 contains the supplementary crystallographic data for **1**-**5**. These data can be obtained free of charge via http://www.ccdc.cam.ac.uk/conts/retrieving.html, or from the Cambridge Crystallographic Data Centre, 12 Union Road,Cambridge CB2 1EZ, UK; fax: +44 1223 336 033; or e-mail: deposit@ccdc.cam.ac.uk.

Acknowledgements

The financial support of the University Grants Commission, New Delhi, India (F. No. 42-396/2013 (SR) TSBB) and the Indo-Swiss Joint Research Programme, Joint Utilisation of Advanced Facilities (Grant No. JUAF 11, TSBB, AL) are gratefully acknowledged. Support from the Ministry of Higher Education, Malaysia, and the University of Malaya, for High Impact Research grant (UM.C/HIR-MOHE/SC/03) is also gratefully acknowledged. The authors gratefully acknowledge for the access to the X-ray facilities in the Chemical Research Center at the Autonomous State University of Morelos (CIQ-UAEM).

References

[1] E.F. DiMauro, M.C. Kozlowski. *Org. Lett.*, **3**, 1641 (2001).

[2] R. Clérac, H. Miyasaka, M. Yamashita, C. Coulon. *J. Am. Chem. Soc*., **124**, 12837 (2002).

[3] M.R. Maurya, A. Kumar, A.R. Bhat, A. Azam, C. Bader, D. Rehder. *Inorg. Chem*., **45**, 1260 (2006).

[4] T. Glaser, I. Liratzis, O. Kataeva, R. Fröhlich, M. Píacenza, S. Grimme. *Chem. Commun*., 1024 (2006).

[5] A.R. Stefankiewicz, M. Wałesa-Chorab, H.B. Szcześniak, V. Patroniak, M. Kubicki, Z. Hnatejko, J. Harrowfield. *Polyhedron*, **29**, 178 (2010).

[6] T. Katsuki. *Coord. Chem. Rev*., **140**, 189 (1995).

[7] P.J. Pospisil, D.H. Carsten, E.N. Jacobsen. *Chem. Eur. J*., **2**, 974 (1996).

[8] T. Thanyasiri, E. Sinn. *J. Chem. Soc., Dalton Trans*., 1187 (1989).

[9] L. Canali, D.C. Sherrington. *Chem. Soc. Rev*., **28**, 85 (1999).

[10] T.S. Basu Baul, S.Kundu, S. Mitra, H. Höpfl, E.R.T. Tiekink, A. Linden. *Dalton Trans*., **42**, 1905 (2013).

[11] T.S. Basu Baul, S. Kundu, H. Höpfl, E.R.T. Tiekink, A. Linden. *Polyhedron*, **55**, 270 (2013).

[12] A.J. Bloodworth. *J. Organomet. Chem*., **23**, 27 (1970).

[13] *CrysAlisPro*, Version 1.171.33.55, Agilent Technologies, Yarnton, Oxfordshire, England (2010).

[14] R. Hooft. *KappaCCD Collect Software*, Nonius BV, Delft, The Netherlands (1999).

[15] Bruker Analytical X-ray Systems, SAINT-NT Version 6.04 (2001).

[16] Z. Otwinowski, W. Minor. *Methods in Enzymology*, in: C.W. Carter Jr., R.M. Sweet (Eds.), Macromolecular Crystallography, Part A, vol. 276, Academic Press, New York, pp. 307-326 (1997).

[17] R.H. Blessing, *Acta Crystallogr*., Sect A, **51**, 33 (1995).

[18] R.C. Clark, J.S. Reid, *Acta Crystallogr*., Sect. A, **51**, 887 (1995).

[19] P.T. Beurskens, G. Admiraal, G. Beurskens, W.P. Bosman, S. Garcia-Granda, R.O. Gould, J.M.M. Smits, C. Smykalla. PATTY: The DIRDIF Program System, Technical Report of the Crystallography Laboratory, University of Nijmegen, The Netherlands (1992).

[20] Bruker Analytical X-ray Systems, SHELXTL-NT Version 6.10 (2000).

[21] G. M. Sheldrick. *Acta Crystallogr*., Sect. A, **64**, 112 (2008).

[22] S.S. Tandon, S. Chander, L.K. Thompson. *Inorg. Chim. Acta*, **302**, 683 (2000).

[23] K. Nakamoto. *Infrared and Raman Spectra of Inorganic and Coordination Compounds*, Wiley, New York (1986).

[24] G. Mahmoudi, A. Morsali. *Polyhedron*, **27**, 1070 (2008).

[25] J. Ribas, A. Escuer, M. Monfort, R. Vicente, R. Cortes, L. Lezama, T. Rojo. *Coord. Chem. Rev*., **193-195**, 1027 (1999).

[26] U.S. Ray, B.G. Chand, G.Mostafa, J. Cheng, T.-H. Lu, C. Sinha. *Polyhedron*, **22**, 2587 (2003).

[27] G. J. Kleywegt, W. G. R. Wiesmeijer, G. J. Van Driel, W. L. Driessen, J. Reedijk, J. H. Noordik. *J. Chem. Soc., Dalton Trans*., 2177 (1985).

[28] A.K. Boudalis, V. Nastopoulos, S.P. Perlepes. *Trans. Met. Chem*., **26**, 276 (2001).

[29] P. Biscarini, L. Fusina, G.D. Nivellini. *J. Chem. Soc., Dalton Trans*., 1003 (1972).

[30] K. Nakamoto. *Infrared and Raman Spectra of Inorganic and Coordination Compounds*, Part B, Wiley, Hoboken, New Jersey, 6th Edn. (2009).

[31] T.K. Chattopadhyay, A.K. Kumar, A. Roy, A.S. Batsanov, E.B. Shamuratov, Yu. T. Struchkov. *J. Organomet. Chem*., **419**, 277 (1991).

[32] S. Basu Baul, T.S. Basu Baul, E. Rivarola, D. Dakternieks, E.R.T. Tiekink, A. Chatterjee, C. Sing-ai. *Appl. Organometal. Chem*.,**12**, 503 (1998).

[33] C. Seward, J. Chan, D. Song, S.-N. Wang. *Inorg. Chem*., **42**, 1112 (2003).

[34] a) R.S. Drago. *Physical Methods in Chemistry*, Chap. 5, Saunders, Philadelphia (1977); b) F. Masetti, U. Mazzucato, G. Galiazzo. *J. Lumin*., **4**, 8 (1971); c) T.C. Warner, W. Hawkins, J. Facci, R. Torrisi, T. Trembath. *J. Phys. Chem*., **82**, 298 (1978); d) M.C. Aragoni, M. Arca, F. Demartin, F.A. Devillanova, F. Isaia, A. Garau, V. Lippolis, F. Jalali, U. Papke, M. Shamsipur, L. Tei, A. Yari, G. Verani. *Inorg. Chem*., **41**, 6623 (2002).

[35] A. W. Addison, T. N. Rao, J. Reedijk, J. van Rijn, G. C. Verschoor. *J. Chem. Soc., Dalton Trans*., 1349 (1984).

[36] J. Gans, D. Shalloway. *J. Mol. Graphics Modell*., **19**, 557 (2001).

[37] K. Brandenburg. *DIAMOND*, Crystal Impact GbR, Bonn, Germany (2006).

[38] Z.D. Tomić, D.N. Sredojević, S.D. Zarić. *Cryst. Growth Des*., **6**, 29 (2006).

[39] D.N. Sredojević, Z.D. Tomić, S.D. Zarić. *Cryst. Growth Des*., **10**, 3901 (2010).

[40] E.R.T. Tiekink, in: J.W. Steed, P.A. Gale (Eds.), *Crystal Engineering. Supramolecular Chemistry: From Molecules to Nanomaterials*, John Wiley &Sons Ltd., Chichester, UK, p. 2791 (2012).

Table 1. Crystal data, data collection and refinement parameters for compounds **1-5**.

	1	**2**	**3**	**4**	**5**
Empirical formula	$C_{13}H_{12}Cl_2HgN_2O$	$C_{26}H_{24}Hg_3N_{22}O_2$	$C_{13}H_{12}Cl_2HgN_2O$	$C_{13}H_{12}HgN_4O_7$**.** CH_3CN	$C_{15}H_{18}HgN_4O_8S$
Formula weight	483.74	1278.12	483.77	577.81	614.89
Crystal size (mm)	0.12× 0.14 × 0.49	0.15 × 0.23 × 0.28	0.14 ×0.18 × 0.30	0.05 × 0.18 × 0.30	0.05 × 0.08 × 0.35
Crystal morphology	Block	Prism	Prism	Plate	Needle
Temperature (K)	293(2)	160(1)	160(1)	160(1)	160(1)
Crystal system	orthorhombic	triclinic	monoclinic	orthorhombic	triclinic
Space group	*Pbca*	$P\bar{1}$	$P2_1/c$	*Pbca*	$P\bar{1}$
a (Å)	8.8128(13)	8.50515(18)	9.29317(17)	16.3111(2)	8.0022(1)
b (Å)	21.657(3)	9.7632(3)	7.10215(11)	9.4077(1)	10.2965(2)
c (Å)	30.600(4)	11.5385(3)	20.6719(4)	24.1767(4)	13.0245(3)
α(°)	90	67.645(3)	90	90	112.4632(8)
β(°)	90	79.274(2)	95.0498(17)	90	94.3431(11)
γ(°)	90	82.950(2)	90	90	95.3738(11)
V (Å^3)	5840.3(15)	869.22(4)	1359.08(4)	3709.91(9)	980.09(3)
Z	16	1	4	8	2
D_x (g cm^{-3})	2.201	2.441	2.364	2.069	2.083
μ (mm^{-1})	10.899	13.307	11.734	8.365	8.027
θrange(°)	2.3–25.0	2.3–32.5	2.2–29.5	2.5–27.5	2.2–30.1
Reflections measured	40015	21265	15755	53425	22892
Independent reflections; R_{int}	5142; 0.086	5774; 0.038	3405; 0.037	4247; 0.115	5654; 0.074
Reflections with $I > 2\sigma(I)$	3543	5262	3177	2979	5211
Number of parameters	345	243	174	255	266
$R(F)$ [$I > 2\sigma(I)$reflns]	0.037	0.027	0.0277	0.0397	0.0284
$wR(F^2)$ (all data)	0.087	0.069	0.0669	0.1066	0.0637
GOF(F^2)	1.00	1.10	1.172	1.019	1.074
$\Delta\rho_{max, min}$ (e, Å^{-3})	0.84, -0.59	2.89, -1.54	2.14, -1.15	2.16, -1.82	1.28, -1.45

Table 2. Photophysical data for compounds **1-5** in acetonitrile solution.

Compounds	Electronic spectroscopic data λ_{max} (nm); (ε[$M^{-1}cm^{-1}$])	Photoluminescence data λ_{em}(nm)[a]	ϕ_F
1	359 (12,096)	413,427, 502	0.11
2	346 (22,109)	413,429	0.08
3	378 (17,937)	412, 430	0.10
4	382 (11,390)	411, 431	0.12
5	382 (9,305)	412,429	0.09

[a]The long wavelength emission appears as a shoulder in all cases.

Table 3. Selected bond lengths (Å) and angles (º) for **1** and **3**.[a]

	1	**3**		**1**	**3**
Hg(1)-Cl(1)	2.374(2)	2.4061(12)	Cl(2)-Hg(1)-N(1)	91.02(18)	98.89(10)
Hg(1)-Cl(2)	2.446(2)	2.5597(11)	Cl(2)-Hg(1)-N(2)	114.90(15)	100.07(9)
Hg(1)-N(1)	2.324(6)	2.260(4)	N(1)-Hg(1)-N(2)	69.1(2)	69.99(13)
Hg(1)-N(2)	2.473(6)	2.557(4)	Cl(1)-Hg(1)-Cl(2')	-	95.09(4)
Hg(1)-Cl(2')	-	2.7874(11)	Cl(2)-Hg(1)-Cl(2')	-	100.77(2)
C(1)-C(6)	1.449(12)	1.454(7)	N(1)-Hg(1)-Cl(2')	-	88.32(10)
N(2)-C(6)	1.259(10)	1.287(6)	N(2)-Hg(1)-Cl(2')	-	151.92(9)
N(2)-C(7)	1.406(10)	1.422(6)	Hg(1)-Cl(2)-Hg(1")	-	128.57(5)
			Hg(1)-N(1)-C(1)	118.4(6)	119.1(3)
Cl(1)-Hg(1)-Cl(2)	125.35(8)	106.62(4)	Hg(1)-N(1)-C(5)	122.3(6)	121.8(3)
Cl(1)-Hg(1)-N(1)	139.01(17)	153.09(10)	Hg(1)-N(2)-C(6)	113.6(6)	110.7(3)
Cl(1)-Hg(1)-N(2)	105.06(17)	96.77(9)	Hg(1)-N(2)-C(7)	124.2(5)	128.0(3)

[a] Symmetry operations for primed and doubly-primed atoms = 1-*x*, ½+*y*, 1½-*z* and 1-*x*, -½+*y*, 1½-*z*, respectively.

Table 4. Selected bond lengths (Å) and angles (º) for **2**.[a]

	2		**2**
Hg(1)-N(1)	2.402(3)	N(1)-Hg(1)-O(1)	120.51(8)
Hg(1)-N(2)	2.453(3)	N(2)-Hg(1)-N(3)	92.00(10)
Hg(1)-N(3)	2.184(3)	N(2)-Hg(1)-N(6)	119.65(11)
Hg(1)-N(6)	2.138(3)	N(2)-Hg(1)-N(3')	141.38(8)
Hg(1)-N(3')	2.806(3)	N(2)-Hg(1)-O(1)	58.11(7)
Hg(1)-O(1)	2.926(2)	N(3)-Hg(1)-N(6)	137.83(12)
Hg(2)-N(6)	2.710(3)	N(3)-Hg(1)-N(3')	77.25(10)
Hg(2)-N(9)	2.069(3)	N(3)-Hg(1)-O(1)	94.72(9)
Hg(2)-N(5')	2.756(3)	N(6)-Hg(1)-N(3')	90.67(10)
		N(6)-Hg(1)-O(1)	81.62(10)
N(1)-Hg(1)-N(2)	68.71(9)	N(3')-Hg(1)-O(1)	158.05(8)
N(1)-Hg(1)-N(3)	112.62(9)	N(6)-Hg(2)-N(9)	94.56(13)
N(1)-Hg(1)-N(6)	105.01(11)	N(6)-Hg(2)-N(5')	87.87(10)
N(1)-Hg(1)-N(3')	81.31(9)	N(9)-Hg(2)-N(5')	90.25(11)

[a] Symmetry operation for primed atoms = 1-*x*, -*y*, 1-*z*.

Table 5. Selected bond lengths (Å) and angles (º) for **4** and **5**.[a]

	4	**5**		**4**	**5**
Hg(1)-O(2)	2.757(5)	2.623(3)	O(3)-Hg(1)-O(5)	80.86(14)	74.57(11)
Hg(1)-O(3)	2.157(4)	2.599(3)	O(3)-Hg(1)-O(7)	85.10(15)	119.40(10)
Hg(1)-O(5)	2.731(4)	2.393(3)	O(3)-Hg(1)-N(1)	167.09(17)	138.07(10)
Hg(1)-O(7)	2.587(4)	2.712(3)	O(3)-Hg(1)-N(2)	118.92(17)	95.54(10)
Hg(1)-N(1)	2.200(5)	2.259(3)	O(5)-Hg(1)-O(7)	47.92(12)	49.40(11)
Hg(1)-N(2)	2.398(4)	2.431(3)	O(5)-Hg(1)-N(1)	103.97(15)	102.67(11)
C(1)-C(6)	1.487(8)	1.473(5)	O(5)-Hg(1)-N(2)	90.15(15)	160.11(11)
N(2)-C(6)	1.272(7)	1.277(5)	O(7)-Hg(1)-N(1)	89.37(16)	82.30(11)
N(2)-C(7)	1.416(7)	1.417(4)	O(7)-Hg(1)-N(2)	129.66(14)	144.86(10)
Hg(1)-O(x)	2.924(4)	2.229(3)	N(1)-Hg(1)-N(2)	73.41(16)	72.93(10)
Hg(1)-O(6')	2.725(4)	-	O(2)-Hg(1)-O(x)	100.03(12)	129.49(10)
			O(3)-Hg(1)-O(x)	84.22(14)	80.66(10)
O(2)-Hg(1)-O(3)	50.81(15)	49.04(9)	O(5)-Hg(1)-O(x)	115.21(11)	95.82(11)
O(2)-Hg(1)-O(5)	116.33(13)	77.18(11)	O(7)-Hg(1)-O(x)	68.28(12)	83.68(11)
O(2)-Hg(1)-O(7)	135.80(14)	121.49(10)	N(1)-Hg(1)-O(x)	82.89(14)	140.24(11)
O(2)-Hg(1)-N(1)	132.82(16)	89.17(10)	N(2)-Hg(1)-O(x)	149.00(12)	99.58(10)
O(2)-Hg(1)-N(2)	82.62(15)	83.31(10)	O(2)-Hg(1)-O(6')	69.77(13)	-
O(3)-Hg(1)-O(6')	90.24(15)	-	O(5)-Hg(1)-O(6')	159.46(11)	-
O(7)-Hg(1)-O(6')	113.22(13)	-	N(1)-Hg(1)-O(6')	81.22(14)	-
N(2)-Hg(1)-O(6')	110.32(13)	-	O(x)-Hg(1)-O(6')	45.00(11)	-

[a] x = 5' for **4** and x = 8 for **5**. Symmetry operation for primed atoms = -*x*, -½+*y*, ½-*z*.

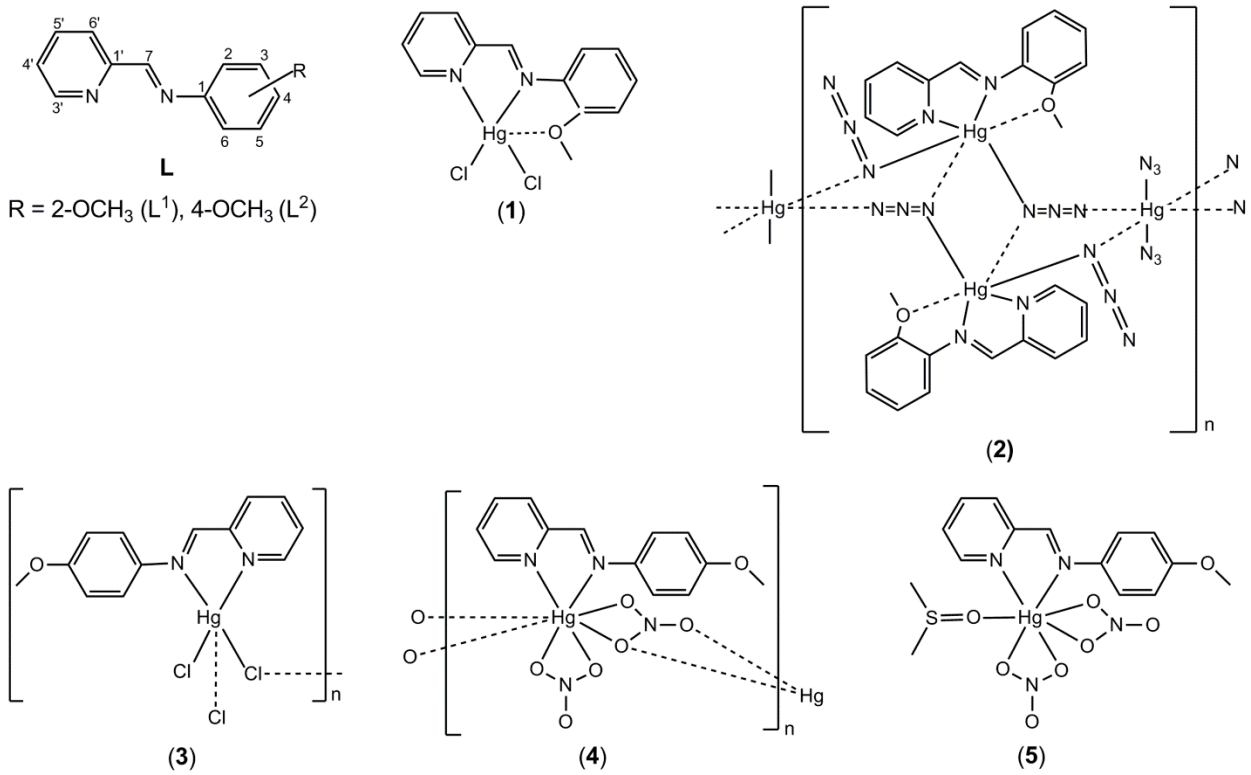

Scheme 1. The ligands L^1-L^2 and the investigated compounds **1-5**

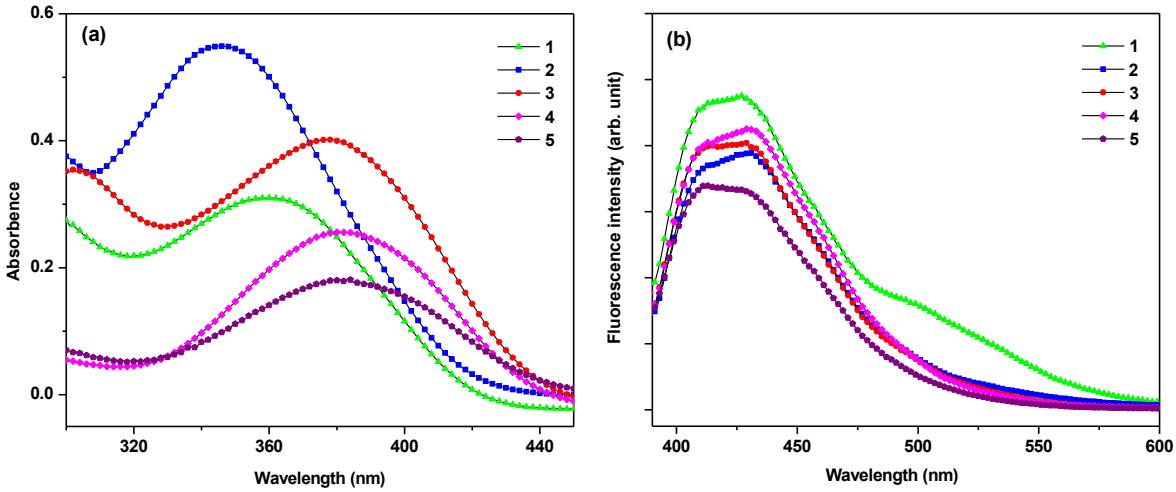

Figure 1. (a) UV–Vis (concentration 10^{-3}M) and (b) fluorescence spectra (concentration ~10^{-5} M) obtained by excitation at the respective absorption maxima (Table 2) of compounds **1-5** in acetonitrile solution.

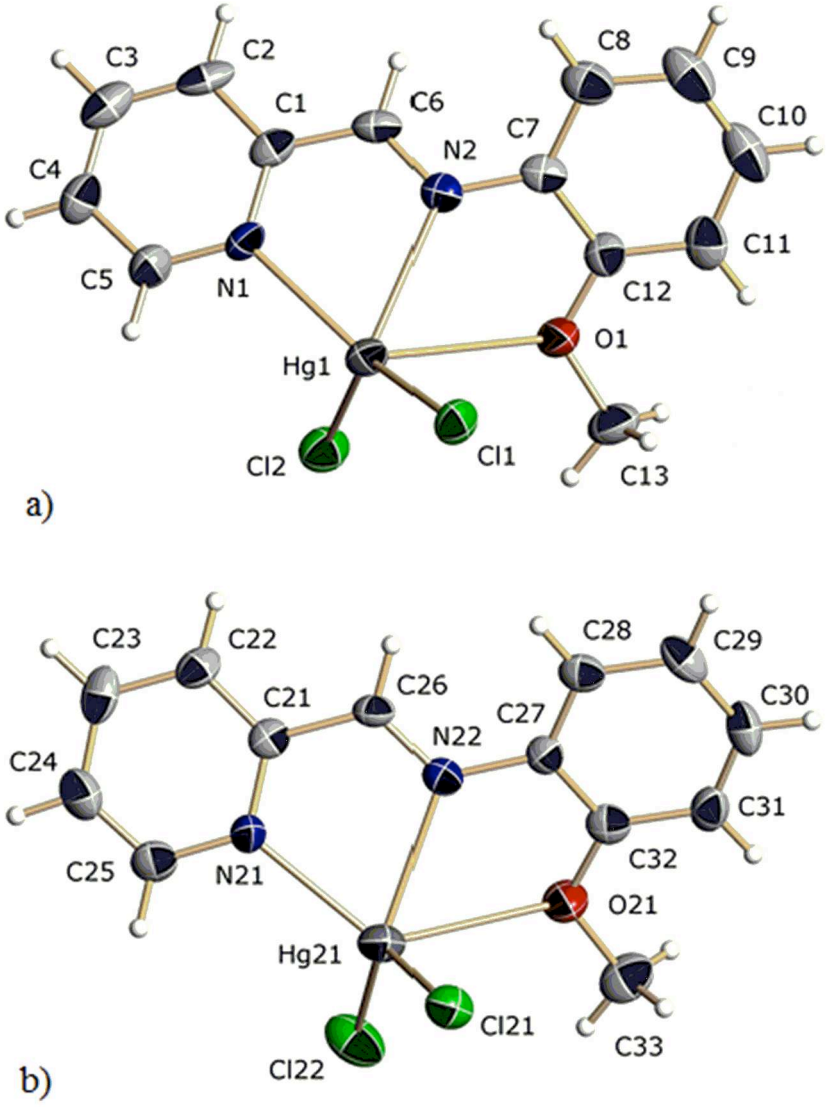

Figure 2. Perspective views of the two crystallographically independent monomers (a and b) found in the crystal structure of $[HgL^1(Cl)_2]$ (**1**). Displacement ellipsoids are drawn at the 30% probability level and H atoms are shown as small spheres of arbitrary radii.

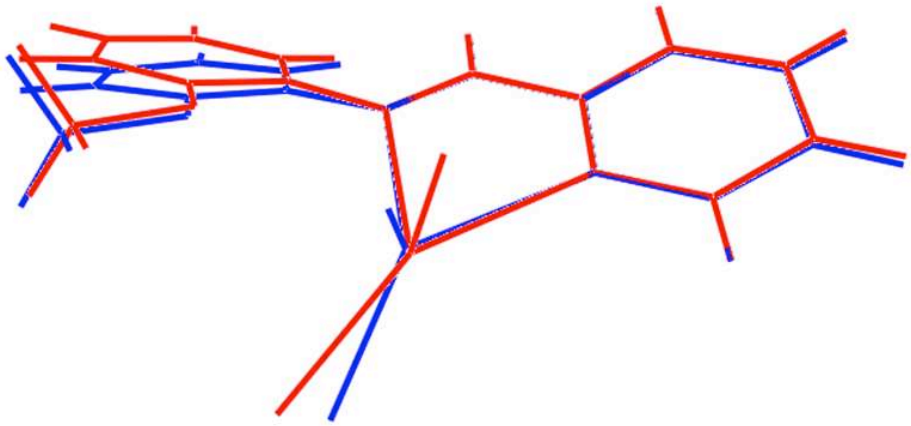

a)

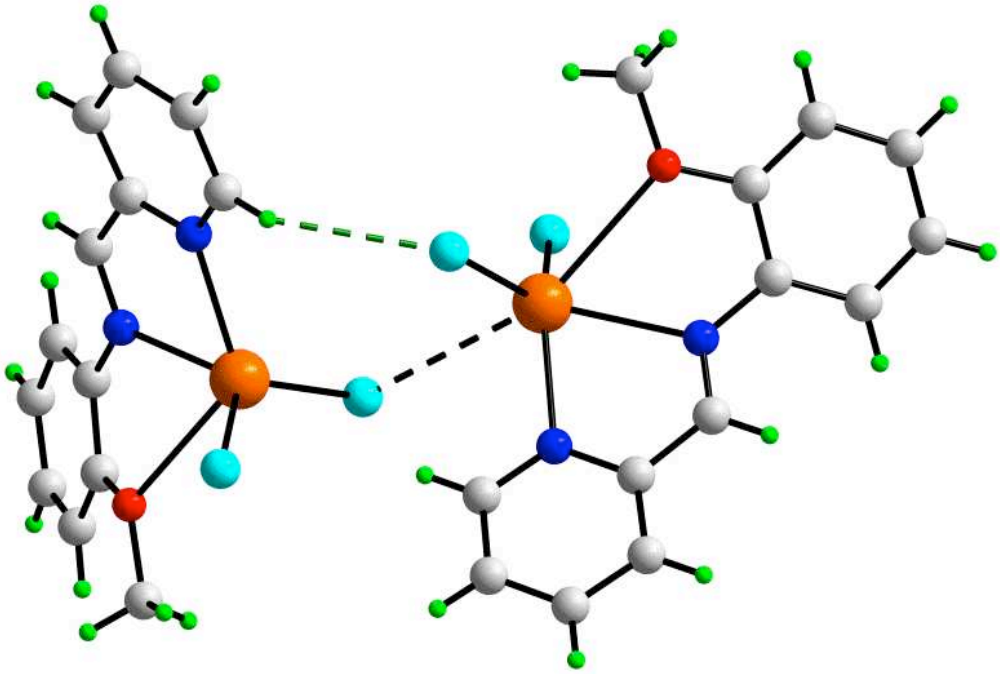

b)

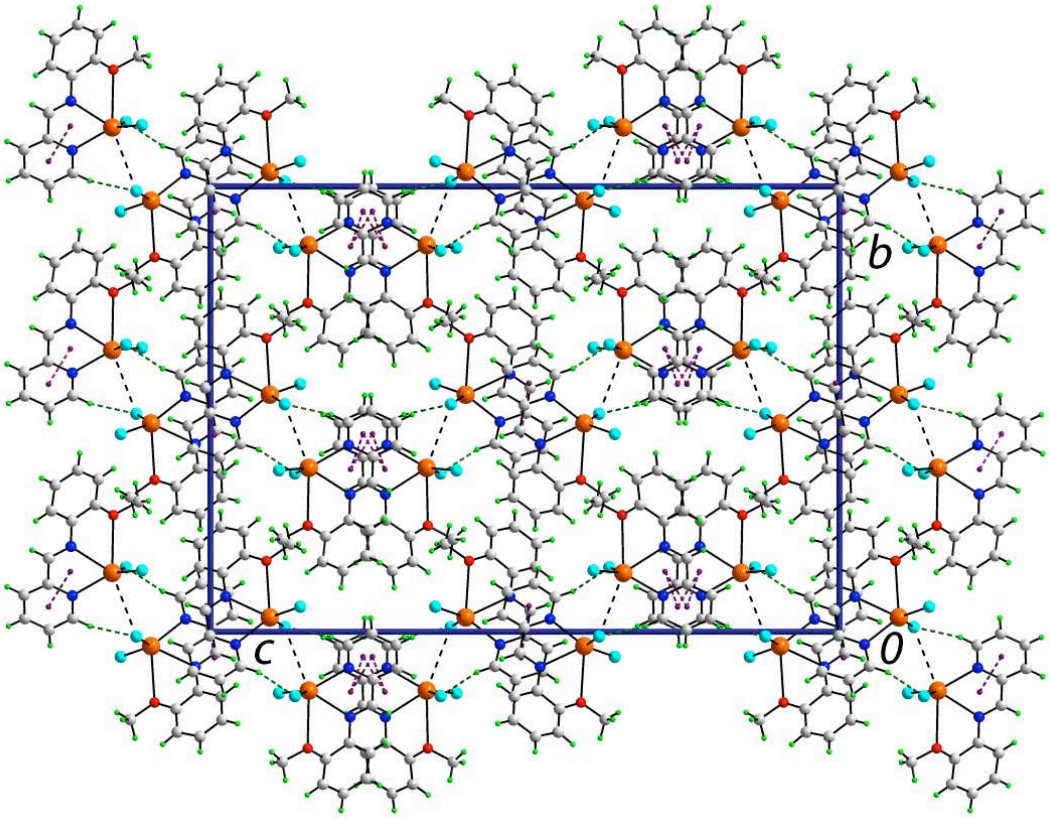

c)

Figure 3. (a) Overlay diagram of the two independent molecules in [$HgL^1(Cl)_2$] (**1**) (red image contains Hg1) which have been superimposed so that the HgN_2C_2 rings are overlapped. (b) Illustration of the secondary Hg...Cl bonding [black dashed line, 3.309(2) Å] connecting the two independent molecules as well as the C-H...Cl hydrogen bond [green dashed line; H...Cl = 2.79 Å]. (c) View in projection down the a-axis of the unit cell contents. The C-H...Cl hydrogen bonds [C5-H5...Cl21^{i}: H5...Cl21^{i}= 2.82 Å, C5...Cl21^{i} = 3.502(10) Å, angle at H5 = 131º for i: -1+*x*, -1+*y*, *z*; C25-H25...Cl2^{ii}: H25...Cl2^{ii}= 2.79 Å, C25...Cl2^{ii} = 3.467(9) Å, angle at H25 = 130º for ii: 1+*x*, 1+*y*, *z*] and π□π interactions [Cg(N21,C21-C25)...Cg(N21,C21-C25)^{iii} = 3.484(5) Å for iii: 1-*x*, 2-*y*, -*z*; Cg(Hg1,N1,N2,C1,C6)...Cg(N1,C1-C5)^{iv} = 3.744(5) Å, angle of inclination =

7.9(4)º for iv: ½+*x*, *y*, ½-*z*] are shown as green and purple dashed lines, respectively. (Colour online.)

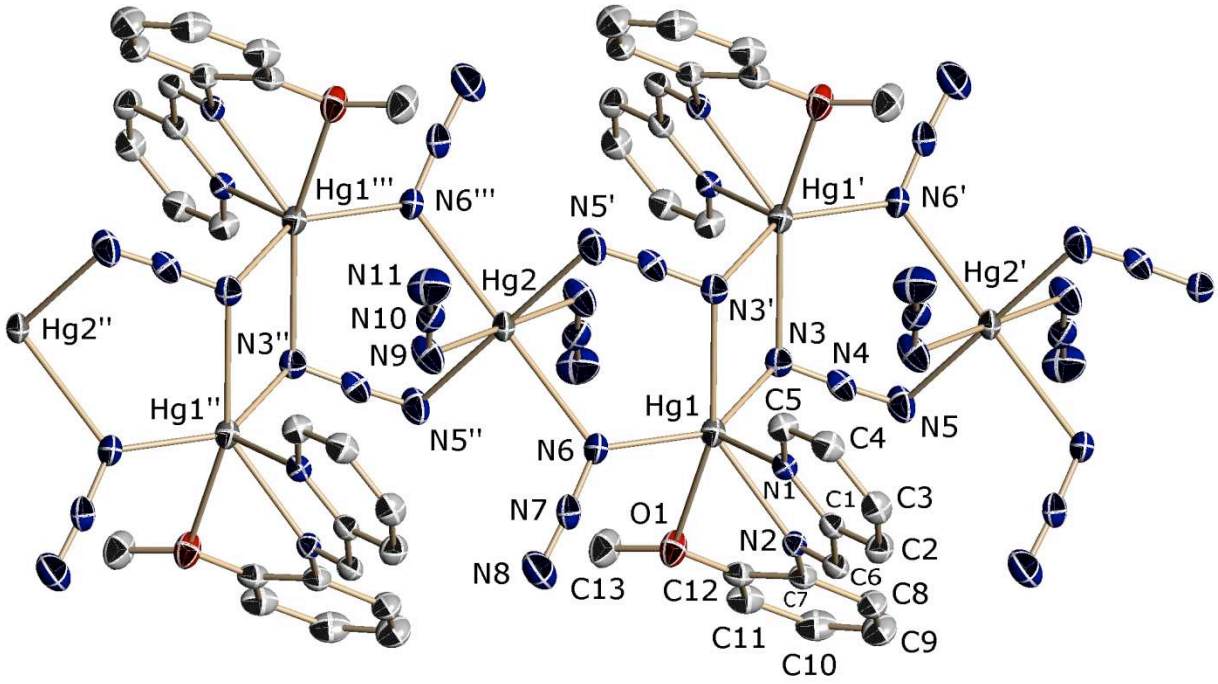

Figure 4. Perspective view of the polymeric chain found in the crystal structure of $\{[HgL^1(N_3)_2]_2 \cdot Hg(N_3)_2\}_n$ (**2**). Displacement ellipsoids are drawn at the 50% probability level and H atoms are omitted. Singly, doubly and triply primed atoms are related by the symmetry operations 1-*x*, -*y*, 1-*z*, 1+*x*, *y*, *z* and 2-*x*, -*y*, 1-*z*, respectively.

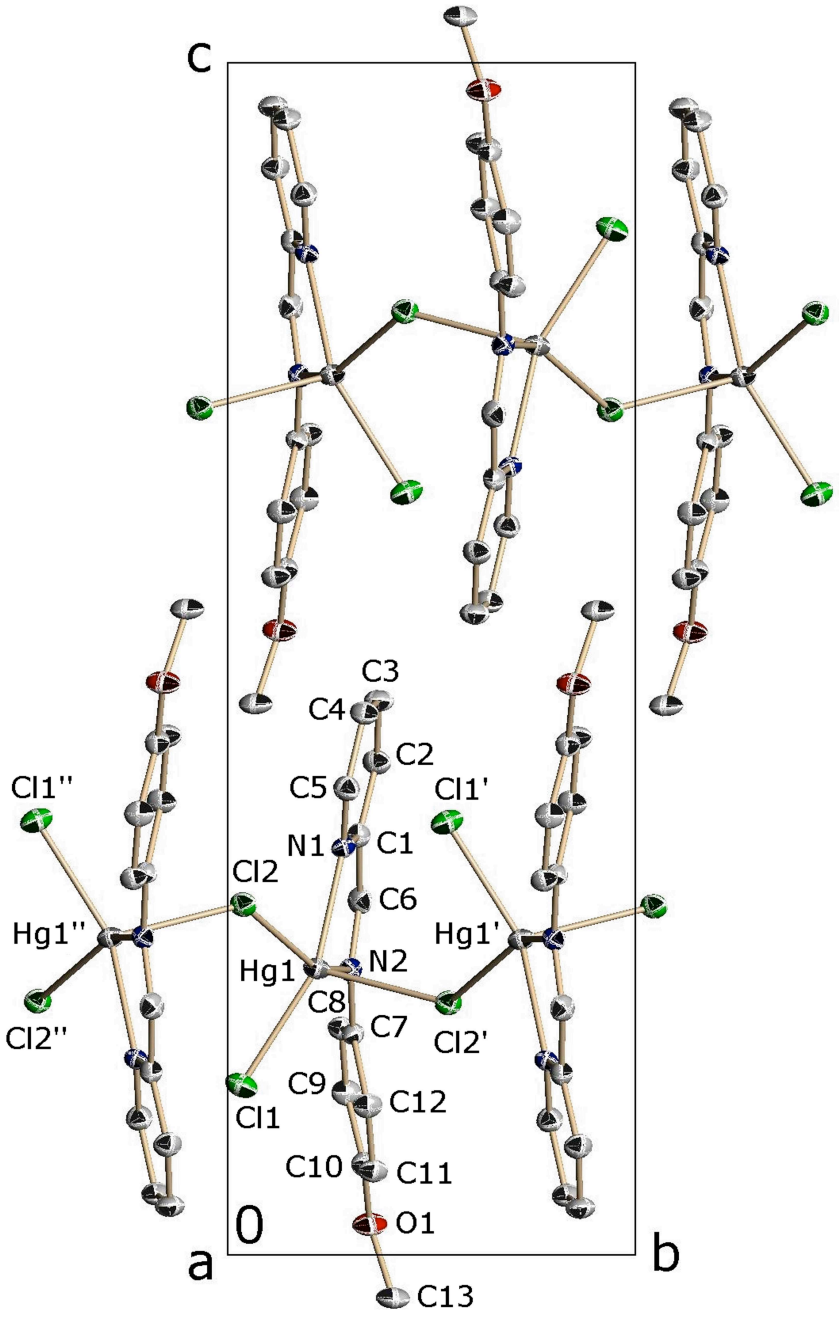
c
a
b
0
C3
C4
C2
C5
Cl1''
Cl1'
N1
C1
Cl2
C6
Hg1''
Hg1'
Hg1
N2
C8
C7
Cl2''
Cl2'
C9
C12
Cl1
C10
C11
O1
C13

a)

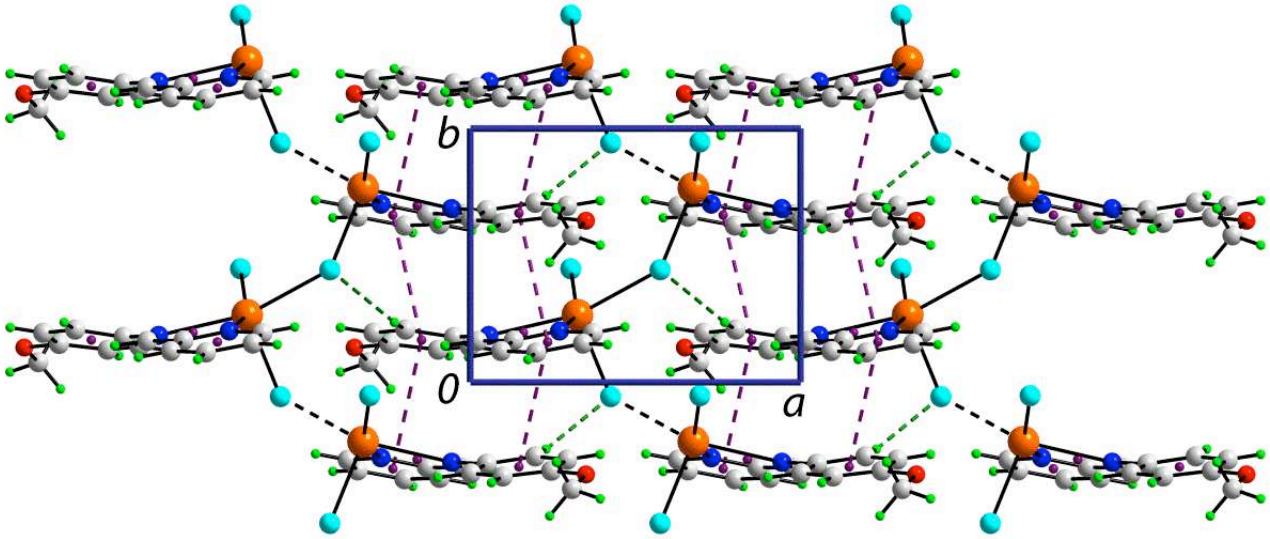

b)

Figure 5. (a) View down the a-axis of the unit cell contents of $[HgL^2(Cl)_2]_n$ (**3**) showing the weakly associated extended chain. Displacement ellipsoids are drawn at the 50% probability level and H atoms are omitted. The primed and doubly primed atoms are related by the symmetry operations 1-*x*, ½+*y*, 1½-*z* and 1-*x*, -½+*y*, 1½-*z*, respectively (b) A view of the supramolecular layer in the ab-plane sustained by C-H...Cl hydrogen bonds [C8-H8...$Cl2^i$: H8...$Cl2^i$= 2.73 Å, C8...$Cl2^i$ = 3.543(5) Å, angle at H5 = 144º for i: 2-*x*, ½+*y*, 1½-*z*] and π-π interactions [Cg(N1,C1-C5)...$Cg(C7-C12)^{ii,iii}$ = 3.631(3) Å and 3.738(3) Å, angle of inclination = 2.2(2)º in each case, for ii: 2-*x*, -½+*y*, -1½-*z*; and iii: 2-*x*, ½+*y*, 1½-*z*] are shown as green and purple dashed lines, respectively. (Colour online.)

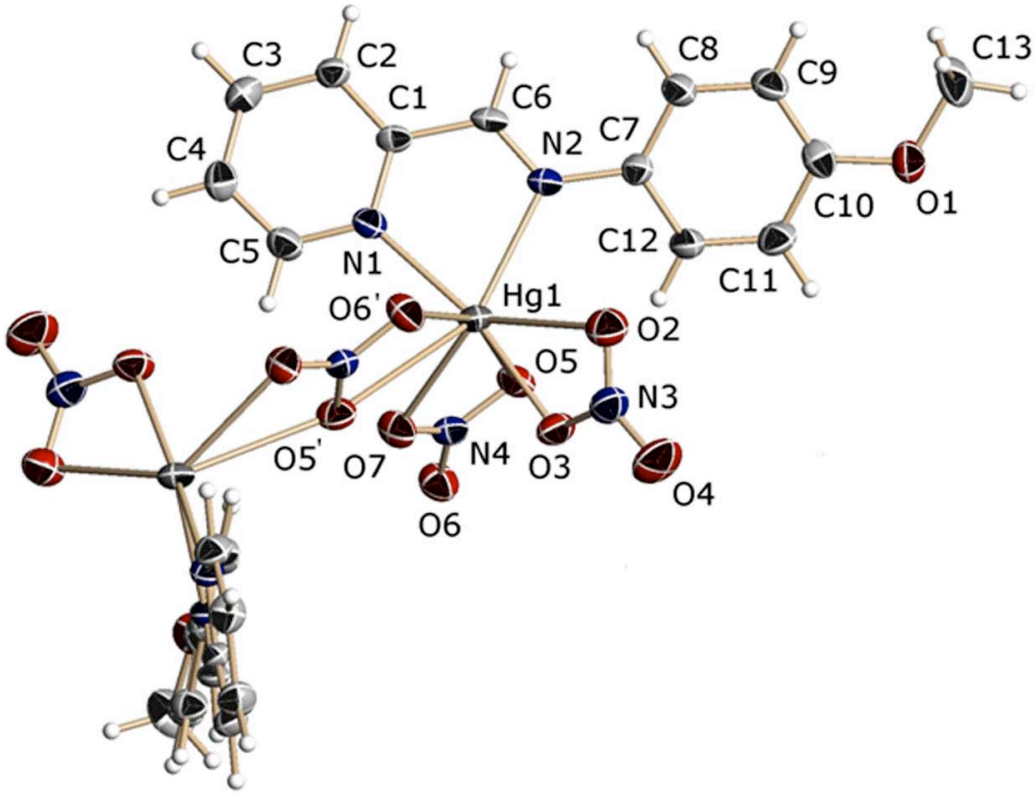
C3
C2
C1
C6
C8
C9
C13
C4
N2
C7
C10
O1
C5
N1
C12
C11
O6'
Hg1
O2
O5
N3
O5'
O7
N4
O3
O4
O6

a)

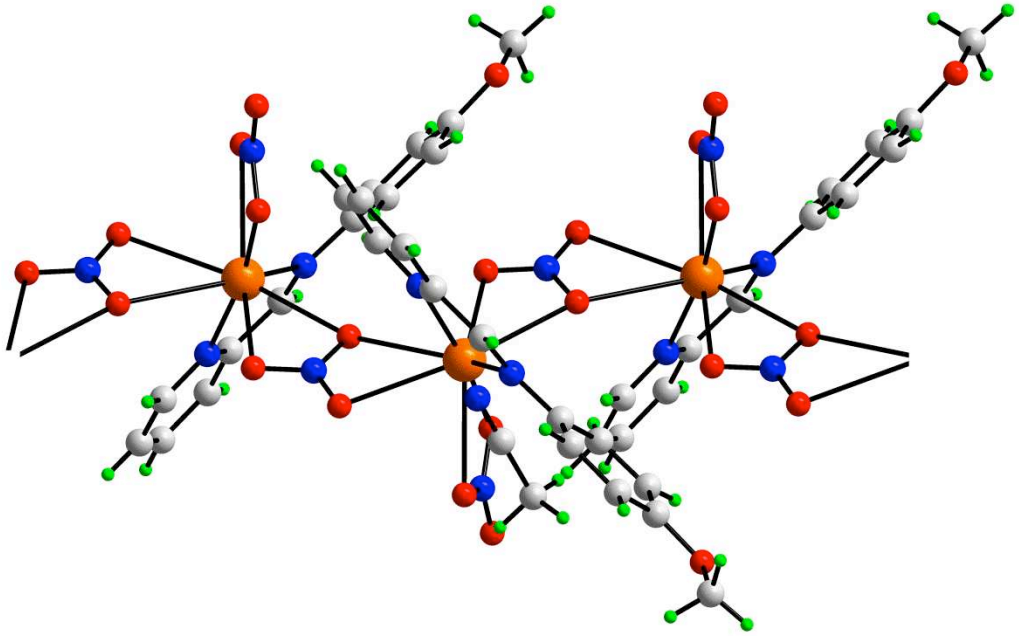

b)

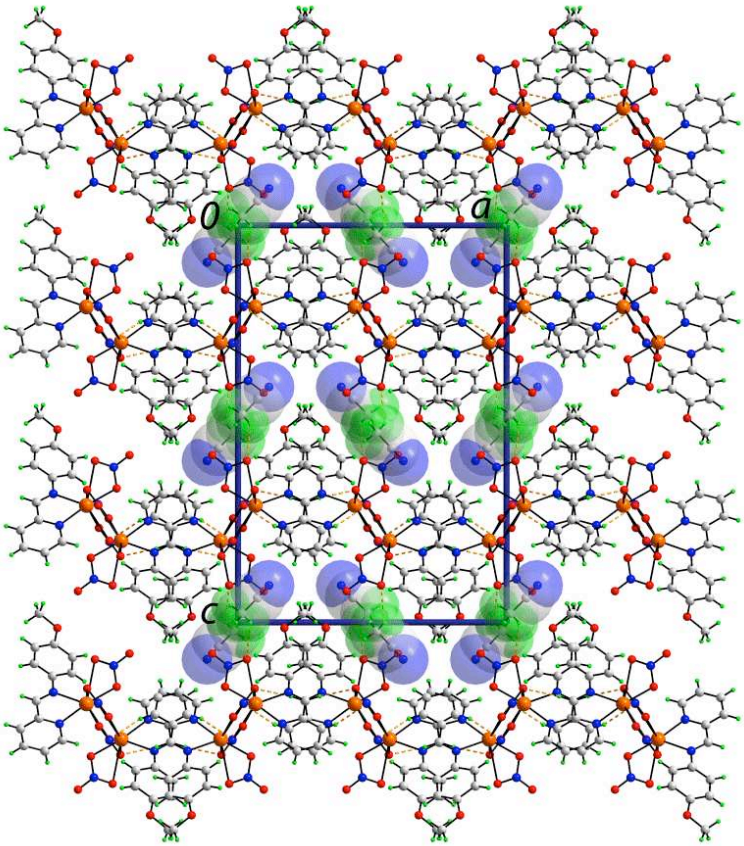

c)

Figure 6. (a) Perspective view of a portion of the polymeric chain illustrated to show the coordination geometry about the mercury(II) atom found in the crystal structure of $[HgL^2(NO_3)_2]_n \cdot nCH_3CN$ (**4**); the acetonitrile molecule is omitted. Displacement ellipsoids are drawn at the 50% probability level and H atoms are shown as small spheres of arbitrary radii. Primed atoms are related by the symmetry operation *-x*, -½+*y*, ½-*z*. (b) The helical coordination polymer mediated by tetradentate nitrate anions. (c) A view in projection down the b-axis of the unit cell contents. The supramolecular layers are sustained by C-H...O interactions [C2-H2...O7^i: H2...O7^i= 2.50 Å, C2...O7^i = 3.413(7) Å, angle at H2 = 162º; C6-H6...O6^i: H6...O6^i= 2.59 Å, C6...O6^i = 3.515(6) Å, angle at H6 = 165º for i: ½+*x*, *y*, ½-*z*] shown as orange dashed lines. The acetonitrile molecules, shown in space-filling mode, are connected to the layers by methyl-C-

H...O(nitrate) interactions [C14-H142...O2^{ii}: H142...O2^{ii}= 2.56 Å, C14...O2^{ii} = 3.381(9) Å, angle at H142 = 141º for ii: ½+*x*, ½-*y*, -*z*]. (Colour online.)

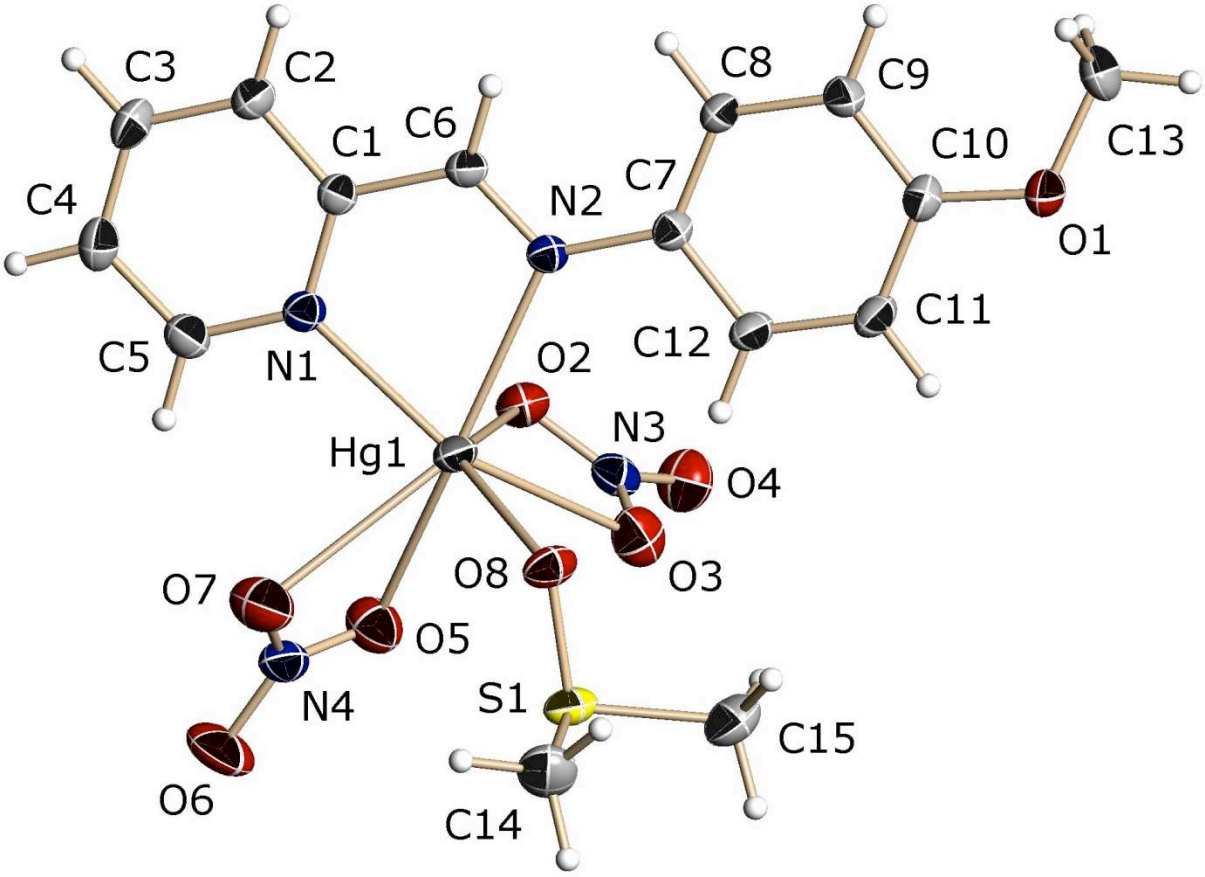
C3
C2
C1
C6
C8
C9
C10
C13
C4
N2
C7
O1
C5
N1
O2
C12
C11
Hg1
N3
O4
O7
O8
O3
O5
N4
S1
C15
O6
C14

a)

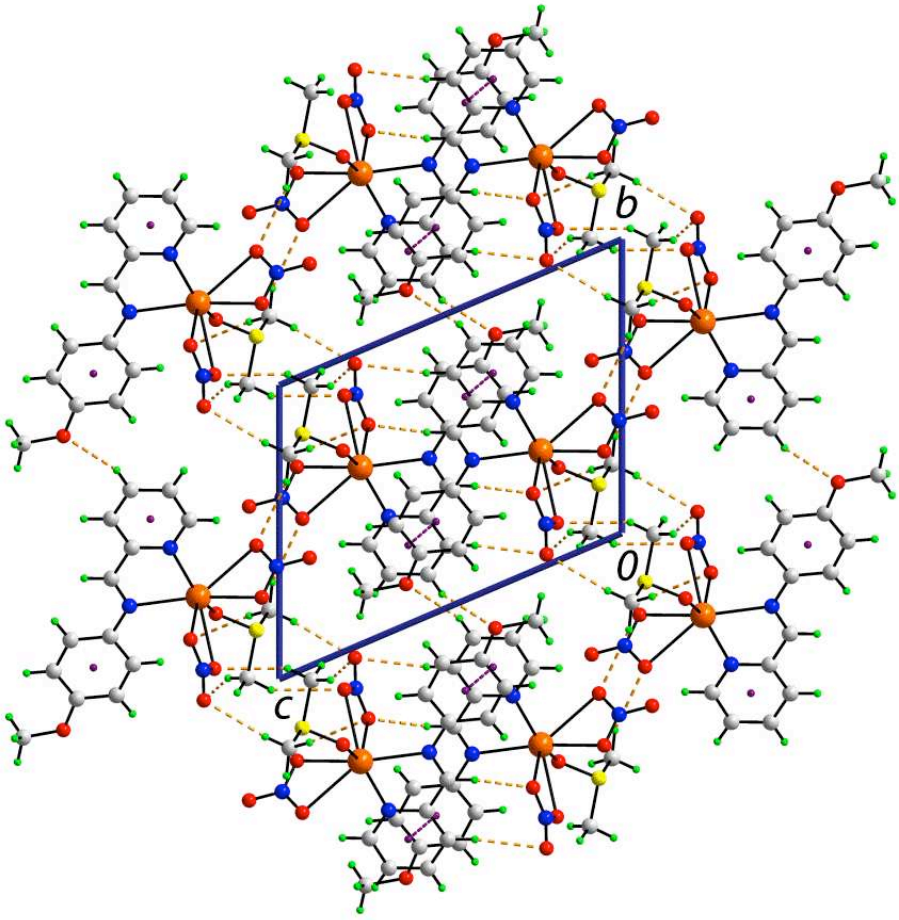

b)

Figure 7. (a) Perspective view of the monomer found in the crystal structure of [$HgL^2(NO_3)_2$(DMSO)] (**5**). Displacement ellipsoids are drawn at the 50% probability level and H atoms are shown as small spheres of arbitrary radii. (b) A view in projection down the a-axis of the unit cell contents. The π-π interactions [Cg(N1,C1-C5)...Cg(C7-C12)^{i} = 3.763(2) Å, angle of inclination = 2.05(19)º for i: 1-*x*, 1-*y*, 1-*z*] are shown as purple dashed lines. The C-H...O interactions [C3-H3...O1^{ii}: H3...O1^{ii}= 2.60 Å, C3...O1^{ii} = 3.508(5) Å, angle at H3 = 160º; C2-H2...O4^{iii}: H2...O4^{iii}= 2.52 Å, C2...O4^{iii} = 3.463(5) Å, angle at H2 = 173º; C6-H6...O2^{iii}: H6...O2^{iii}= 2.42 Å, C6...O2^{iii} = 3.252(5) Å, angle at H6 = 146º; C14-H142...O4^{iv}: H142...O4^{iv}= 2.51 Å, C14...O4^{iv} = 3.477(6) Å, angle at H142 = 169º; C15-H153...O4^{v}: H153...O4^{v}= 2.50 Å,

C15...O4^{v} = 3.400(6) Å, angle at H153 = 152º. Symmetry operations ii: 1+*x*, 1+*y*, +*z*; iii: 1-*x*, 1-*y*, 1-*z*; iv: -*x*, -*y*, -*z*; v: -1+*x*, +*y*, +*z*] are shown as orange dashed lines. (Colour online.)